CHALMERS
UNIVERSITY OF TECHNOLOGY

Structural and optical properties of GaSbBi/GaSb quantum wells [Invited]

Downloaded from: https://research.chalmers.se, 2026-04-04 00:08 UTC

Citation for the original published paper (version of record):

Yue, L., Chen, X., Zhang, Y. et al (2018). Structural and optical properties of GaSbBi/GaSb quantum wells [Invited]. Optical Materials Express, 8(4): 893-900. http://dx.doi.org/10.1364/OME.8.000893

N.B. When citing this work, cite the original published paper.

research.chalmers.se offers the possibility of retrieving research publications produced at Chalmers University of Technology. It covers all kind of research output: articles, dissertations, conference papers, reports etc. since 2004. research.chalmers.se is administrated and maintained by Chalmers Library

(article starts on next page)

Research Article | Vol. 8, No. 4 | 1 Apr 2018 | OPTICAL MATERIALS EXPRESS 893

Optical Materials EXPRESS

Structural and optical properties of GaSbBi/GaSb quantum wells [Invited]

LI YUE,[1,2,*] XIREN CHEN,[3] YANCHAO ZHANG,[1,4] JAN KOPACZEK,[5] JUN SHAO,[3] MARTA GLADYSIEWICZ,[5] ROBERT KUDRAWIEC [5] XIN OU,[2] AND SHUMIN WANG[1,6,*]

[1]*Key Laboratory of Terahertz Solid-State Technology, CAS, Shanghai Institute of Microsystem and Information Technology, Chinese Academy of Sciences, Shanghai 200050, China*
[2]*State Key Laboratory of Functional Materials for Informatics, Shanghai Institute of Microsystem and Information Technology, Chinese Academy of Sciences, Shanghai 200050, China*
[3]*National Laboratory for Infrared Physics, Shanghai Institute of Technical Physics, Chinese Academy of Sciences, Shanghai 200083, China*
[4]*Department of Physical Science and Technology, Shanghai Tech University, Shanghai 201210, China*
[5]*Faculty of Fundamental Problems of Technology, Wroclaw University of Science and Technology, 50-370 Wroclaw, Wybrzeze Wyspianskiego 27, Poland*
[6]*Department of Microtechnology and Nanoscience, Chalmers University of Technology, Gothenburg SE-41296, Sweden*
[7]*yueli@mail.sim.ac.cn*
[8]*shumin@mail.sim.ac.cn*

Abstract: GaSbBi/GaSb quantum wells (QWs) with Bi content up to 10.1% were grown using molecular beam epitaxy. High crystalline quality and clear interfaces were confirmed by high resolution transmission electron microscopy. The Bi distribution was investigated using energy dispersive X-ray spectroscopy. Room temperature photoluminescence (PL) reveals that the peak energy redshifts at a rate of 32 meV/Bi%, consistent with the theoretical predication using the 8-band ***kp*** model. From the temperature dependent PL, it was found that the temperature-insensitivity of the transition from the GaSbBi QW improved with increasing Bi content.

© 2018 Optical Society of America under the terms of the OSA Open Access Publishing Agreement

OCIS codes: (160.6000) Semiconductor materials; (160.4760) Optical properties; (250.5230) Photoluminescence.

References and links

1. M. K. Rajpalke, W. M. Linhart, M. Birkett, K. M. Yu, D. O. Scanlon, J. Buckeridge, T. S. Jones, M. J. Ashwin, and T. D. Veal, "Growth and properties of GaSbBi alloys," Appl. Phys. Lett. **103**(14), 142106 (2013).
2. J. Kopaczek, R. Kudrawiec, W. M. Linhart, M. K. Rajpalke, K. M. Yu, T. S. Jones, M. J. Ashwin, J. Misiewicz, and T. D. Veal, "Temperature dependence of the band gap of $GaSb_{1-x}Bi_x$ alloys with $0 < x \leq 0.042$ determined by photoreflectance," Appl. Phys. Lett. **103**(26), 261907 (2013).
3. M. Gladysiewicz, R. Kudrawiec, and M. S. Wartak, "Electronic band structure and material gain of III-V-Bi quantum wells grown on GaSb substrate and dedicated for mid-infrared spectral range," J. Appl. Phys. **119**(7), 075701 (2016).
4. T. Hosoda, G. Kipshidze, G. Tsvid, L. Shterengas, and G. Belenky, "Type-I GaSb-Based Laser Diodes Operating in 3.1 to 3.3 μm Wavelength Range," IEEE Photonic. Tech. L. **22**(10), 718–720 (2010).
5. L. Shterengas, G. Belenky, T. Hosoda, G. Kipshidze, and S. Suchalkin, "Continuous wave operation of diode lasers at 3.36 μm at 12°C," Appl. Phys. Lett. **93**(1), 011103 (2008).
6. L. Shterengas, G. L. Belenky, J. G. Kim, and R. U. Martinelli, "Design of high-power room-temperature continuous-wave GaSb-based type-I quantum-well lasers with λ > 2.5 μm," Semicond. Sci. Technol. **19**(5), 655–658 (2004).
7. R. Kudrawiec, G. Sek, K. Ryczko, J. Misiewicz, and A. Forchel, "Infrared photomodulation spectroscopy of an $In_{0.22}Ga_{0.78}Sb$/GaSb single quantum well," Superlattices Microstruct. **32**(1), 19–23 (2002).
8. Y. Song, S. Wang, I. Saha Roy, P. Shi, and A. Hallen, "Growth of $GaSb_{1-x}Bi_x$ by molecular beam epitaxy," J. Vac. Sci. Technol. **B30**, 02B114 (2012).
9. S. K. Das, T. D. Das, S. Dhar, M. de la Mare, and A. Krier, "Near infrared photoluminescence observed in dilute GaSbBi alloys grown by liquid phase epitaxy," Infrared Phys. Technol. **55**(1), 156–160 (2012).
10. M. K. Rajpalke, W. M. Linhart, M. Birkett, K. M. Yu, J. Alaria, J. Kopaczek, R. Kudrawiec, T. S. Jones, M. J. Ashwin, and T. D. Veal, "High Bi content GaSbBi alloys," J. Appl. Phys. **116**(4), 043511 (2014).

#321015 https://doi.org/10.1364/OME.8.000893
Journal © 2018 Received 1 Feb 2018; revised 3 Mar 2018; accepted 8 Mar 2018; published 14 Mar 2018

11. L. Yue, Y. Zhang, F. Zhang, L. Wang, Y. Zhuzhong, J. Liu, and S. Wang, "Structural and optical properties of high Bi content GaSbBi films grown by molecular beam epitaxy," in *2016 Compound Semiconductor Week (CSW) Includes 28th International Conference on Indium Phosphide & Related Materials (IPRM) & 43rd International Symposium on Compound Semiconductors (ISCS)*, 2016), 1–2.
12. L. Yue, X. Chen, Y. C. Zhang, F. Zhang, L. J. Wang, J. Shao, and S. M. Wang, "Molecular beam epitaxy growth and optical properties of high bismuth content $GaSb_{1-x}Bi_x$ thin films," J. Alloys Compd. **742**, 780–789 (2018).
13. O. Delorme, L. Cerutti, E. Tournié, and J. B. Rodriguez, "Molecular beam epitaxy and characterization of high Bi content GaSbBi alloys," J. Cryst. Growth **477**, 144–148 (2017).
14. O. Delorme, L. Cerutti, E. Luna, G. Narcy, A. Trampert, E. Tournié, and J. B. Rodriguez, "GaSbBi/GaSb quantum well laser diodes," Appl. Phys. Lett. **110**(22), 222106 (2017).
15. K. Jan, K. Robert, L. Wojciech, R. Mohana, J. Tim, A. Mark, and V. Tim, "Low- and high-energy photoluminescence from $GaSb_{1-x}Bi_x$ with $0 < x \le 0.042$," Appl. Phys. Express **7**(11), 111202 (2014).
16. S. K. Das, T. D. Das, and S. Dhar, "Effect of post-growth anneal on the photoluminescence properties of GaSbBi," Semicond. Sci. Technol. **29**(1), 015003 (2014).
17. X. R. Chen, Y. X. Song, L. Q. Zhu, Z. Qi, L. Zhu, F. X. Zha, S. L. Guo, S. M. Wang, and J. Shao, "Bismuth Effects on Electronic Levels in GaSb(Bi)/AlGaSb Quantum Wells Probed by Infrared Photoreflectance," Chin. Phys. Lett. **32**(6), 067301 (2015).
18. X. Chen, Y. Song, L. Zhu, S. M. Wang, W. Lu, S. Guo, and J. Shao, "Shallow-terrace-like interface in dilute-bismuth GaSb/AlGaSb single quantum wells evidenced by photoluminescence," J. Appl. Phys. **113**(15), 153505 (2013).
19. P. M. Thibado, B. R. Bennett, B. V. Shanabrook, and L. J. Whitman, "A RHEED and STM study of Sb-rich AlSb and GaSb (0 0 1) surface reconstructions," J. Cryst. Growth **175–176**, 317–322 (1997).
20. J. Shao, W. Lu, X. Lü, F. Yue, Z. Li, S. Guo, and J. Chu, "Modulated photoluminescence spectroscopy with a step-scan Fourier transform infrared spectrometer," Rev. Sci. Instrum. **77**(6), 063104 (2006).
21. J. Shao, W. Lu, G. K. O. Tsen, S. Guo, and J. M. Dell, "Mechanisms of infrared photoluminescence in HgTe/HgCdTe superlattice," J. Appl. Phys. **112**(6), 063512 (2012).
22. M. Lee, D. J. Nicholas, K. E. Singer, and B. Hamilton, "A photoluminescence and Hall effect study of GaSb grown by molecular beam epitaxy," J. Appl. Phys. **59**(8), 2895–2900 (1986).
23. G. Pettinari, H. Engelkamp, P. C. M. Christianen, J. C. Maan, A. Polimeni, M. Capizzi, X. Lu, and T. Tiedje, "Compositional evolution of Bi-induced acceptor states in $GaAs_{1-x}Bi_x$ alloy," Phys. Rev. B **83**(20), 201201 (2011).
24. S. Imhof, A. Thränhardt, A. Chernikov, M. Koch, N. S. Köster, K. Kolata, S. Chatterjee, S. W. Koch, X. Lu, S. R. Johnson, D. A. Beaton, T. Tiedje, and O. Rubel, "Clustering effects in Ga(AsBi)," Appl. Phys. Lett. **96**(13), 131115 (2010).
25. D. L. Sales, E. Guerrero, J. F. Rodrigo, P. L. Galindo, A. Yáñez, M. Shafi, A. Khatab, R. H. Mari, M. Henini, S. Novikov, M. F. Chisholm, and S. I. Molina, "Distribution of bismuth atoms in epitaxial GaAsBi," Appl. Phys. Lett. **98**(10), 101902 (2011).
26. C. M. Krammel, M. Roy, F. J. Tilley, P. A. Maksym, L. Y. Zhang, P. Wang, K. Wang, Y. Y. Li, S. M. Wang, and P. M. Koenraad, "Incorporation of Bi atoms in InP studied at the atomic scale by cross-sectional scanning tunneling microscopy," Phys. Rev. Mater. **1**(3), 034606 (2017).
27. D. S. Jiang, H. Jung, and K. Ploog, "Temperature dependence of photoluminescence from GaAs single and multiple quantum-well heterostructures grown by molecular-beam epitaxy," J. Appl. Phys. **64**(3), 1371 (1988).

1. Introduction

GaSbBi alloy exhibits a bandgap reduction about 30–36 meV/% Bi [1, 2], which makes it very promising for developing mid-infrared laser diodes, photodetectors, solar cells and terahertz devices. By introducing Bi component into GaInAsSb QWs, the valence band offset can be increased and the hole leakage will be suppressed [3], which is the major problem existing in conventional GaInAsSb QW lasers [4–6]. Furthermore, a large bandgap energy reduction with relative small compressive strain can be achieved with Bi incorporation into GaSb, better than the In incorporation into GaSb. In the case of InGaSb/GaSb QW reported by Kudrawiec et al. [7], the incorporation of In induces a bandgap reduction of ~77 meV/% strain, while the incorporation of Bi in GaSbBi yields ~829 meV/% strain, more than an order of magnitude. The strong spin-orbit splitting causes that spin-orbit energy exceeds its bandgap with increasing Bi. In that case the Auger recombination process involving the valence band and the spin-orbit band is expected to be suppressed which is beneficial for making temperature-insensitive laser diodes.

Unlike GaAsBi which has been researched comprehensively, epitaxy of GaSbBi was initiated from 2012 [8, 9]. High quality GaSbBi thin films with Bi contents up to 9.6% were reported in 2014 [1] [10]. In 2016, we reported GaSbBi thin films with Bi contents up to 13%

Optical Materials EXPRESS

by varying the Sb/Ga flux ratio using molecular beam epitaxy (MBE) and observed room temperature (RT) PL with a peak wavelength reaching to 3.0 μm [11, 12]. In 2017, Delorme *et al*. reported the GaSbBi films with a Bi content up to 14% and RT PL emission up to 3.8 μm [13]. They also realized GaSbBi QW laser diodes with continuous-wave lasing at 2.5 μm at 80 K, and pulsed lasing near 2.7 μm at room-temperature [14]. These results demonstrate that dilute bismide antimonide alloys are good candidates for mid-infrared devices. In previous reports, all the optical studies including absorption, photoreflectance and PL have been focused on GaSbBi thin films [2, 15, 16], seldom on GaSbBi QWs [17, 18]. It is very important to understand physical properties of GaSbBi QWs for device applications. In this work, we studied structural and optical properties of GaSbBi/GaSb QWs with a Bi content up to 10.1%.

2. Experiments

GaSbBi/GaSb QWs were grown on Te-doped n-type GaSb substrates using a DCA P600 MBE system, equipped with a valved cracker Sb cell and dual filament effusion cells for Ga and Bi. After the oxide desorption at 660 °C, a 100 nm undoped GaSb buffer layer was grown at 620 °C. Then, the substrate temperature was cooled down to 400 °C to grow the 6 nm GaSbBi QW layer. Finally, a 100 nm top GaSb layer was grown and the temperature was ramped up to 620 °C in the meanwhile. All the substrate temperature was monitored using a thermocouple (TC). The temperature measured by the TC is estimated to be about 110 °C higher than the real temperature, i.e., the real temperature is about 290 °C for the temperature 400 °C measured by TC. This temperature difference value was calibrated by observing the critical temperature of 370 °C at which the reflection high-energy electron diffraction (RHEED) reconstruction pattern transforms from (1 × 3) to (1 × 5) [19]. Three 280 nm thick GaSbBi films were grown with Bi contents of 6.6, 8.3 and 10.1% for different Bi fluxes fixed at 4.1×10^{-8}, 7.2×10^{-8} and 1.2×10^{-7} Torr, respectively. During the growth of GaSbBi, the beam equivalent pressure of Ga and Sb are fixed at 2.2×10^{-7} and 4.4×10^{-7}, respectively, with a growth rate of 0.46 μm/h. Three GaSbBi/GaSb QWs were grown under the same growth conditions as that of GaSbBi films. We consider the Bi content in the GaSbBi QW is equal to that in the GaSbBi film.

The Bi contents of three GaSbBi thin films were determined from high resolution X-ray diffraction (HRXRD) by scanning two symmetric (004) and two asymmetric (115) rocking curves. High resolution transmission electron microscopy (HRTEM) measurements were used to examine crystalline and interface quality for GaSbBi QWs. Energy dispersive X-ray spectroscopy (EDS) mapping and line-scan were performed to investigate the Bi distribution profile in the QW. A 532-nm wavelength laser and a liquid-nitrogen cooled InSb detector were used for PL measurements. Room-temperature PL spectra were measured using a conventional rapid-scan Fourier-transform infrared (FTIR) spectrometer, with a pumping power density about 6×10^3 W/cm^2. For the temperature-dependent PL measurements, modulated PL technique based on a step-scan FTIR spectrometer was applied [20], which removes the environmental disturbance and widens the PL spectral range to the very-long wavelength region [21]. The measured temperature was controlled in a closed-cycle cryostat, and the pumping density was about 750 W/cm^2.

3. Results and discussions

3.1 Structural properties

In order to confirm the Bi incorporation into the QW layer and investigate the Bi distribution, scanning-transmission electron microscope (STEM) and EDS mapping images were measured for the GaSbBi QW with a Bi content of 10.1% as shown in Fig. 1. Figure 1(b) shows clear Bi atoms distribution in the QW layer, confirming Bi incorporation into the QW layer. For the Ga atoms, the intensity of EDS signal in the GaSbBi QW layer region has no

Optical Materials EXPRESS

difference with that in the GaSb layers. Whereas, the Sb distribution in the GaSbBi QW is different from that in the GaSb barriers, indicating that Bi atoms replaced Sb atoms positions after incorporation into GaSb. Figure 2 shows the STEM image and the EDS line scans along the growth direction of the GaSbBi QW with a Bi content of 10.1%. The full width at half maximum (FWHM) of the Bi distribution profile is about 6 nm, in consistent with the nominal QW thickness, meaning that Bi atoms diffusion into the adjacent GaSb barriers is negligible. The Sb distribution profile presents a valley in the QW region, which also confirms that the incorporated Bi atoms replaced the sites of Sb atoms. The HRTEM image as shown in Fig. 3 demonstrates clear GaSbBi/GaSb interfaces and high crystalline quality. The width of the GaSbBi QW is about 6–7 nm, again in consistent well with the designed width. Slight fluctuation is observed on the lower GaSbBi/GaSb interface, which is due to the low temperature growth of GaSb. The low growth temperature leads to a rough surface of GaSb. However, the upper GaSbBi/GaSb interface is smother than the lower one as a result of the Bi surfactant effect.

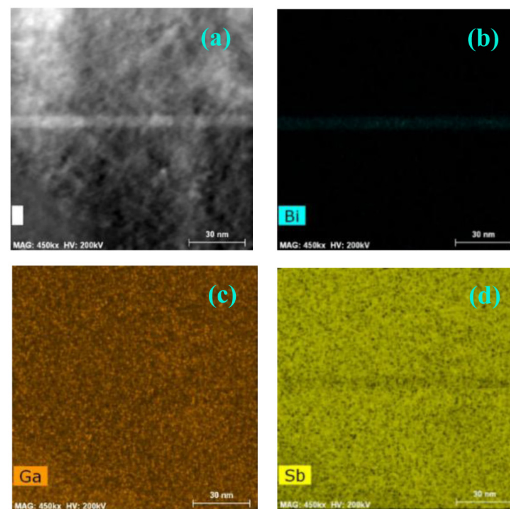

Fig. 1. STEM image (a) and the EDS mappings of (b) Bi, (c) Ga and (d) Sb for GaSbBi QW with Bi content of 10.1%. The scale bar is 30 nm.

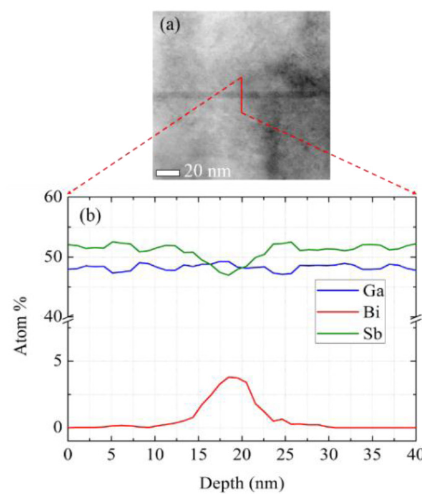

Fig. 2. STEM image (a) and the EDS line scans along the growth direction (b) of the GaSbBi QW with Bi content of 10.1%.

Optical Materials EXPRESS

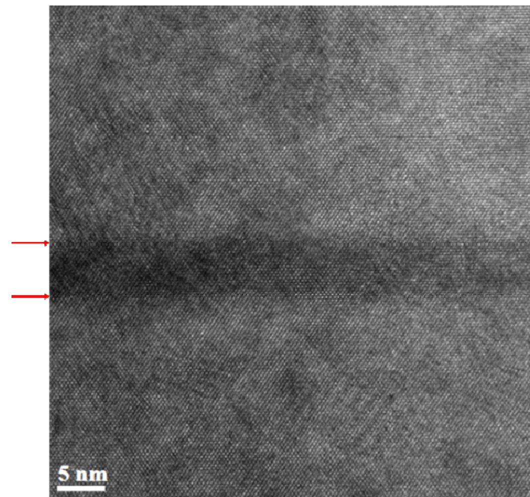

Fig. 3. HRTEM image of the GaSbBi QW with Bi content of 10.1%. The red arrows mark the interfaces.

3.2 Optical properties

Figure 4(a) shows the PL spectra of GaSbBi QWs observed at RT. The left PL peak at 1735 nm is emitted from the GaSb buffer and capping layer. The right PL peak is emitted from the GaSbBi QW. The PL peak redshifts to long wavelength with increasing Bi content, at a redshift rate of 32 meV/Bi%. The PL peak wavelength reaches to 2467 nm for the highest Bi content of 10.1%. With increasing Bi concentration, the PL intensity of GaSbBi QW increases and PL peak becomes broad, whereas the PL intensity of GaSb becomes weak. We believe the broadening of PL is due to the inhomogeneity of Bi distribution in the GaSbBi QW. The Bi distribution becomes more inhomogeneous with increasing Bi concentration. Bi composition fluctuation and Bi atom clusters may exist in high Bi concentration samples. Figure 4(b) shows the extracted PL peak energy (solid squares) together with theoretical calculations performed using the 8-band ***kp*** model (thick black line) [3]. As seen the agreement between experimental data and theoretical calculations is very good, showing the validity of material parameters (band offset, Bi-related reduction of bandgap, etc.) and the model used in the simulation. The band alignment for the three QWs together with confinement energy levels is schematically shown in Fig. 5. It is clearly visible that the quantum confinement for both electrons and holes increases with the increase in Bi concentration. This can explain well why the PL intensity increases with Bi content shown in Fig. 4(a). The thermally induced quenching of PL, which is associated with the electrons (holes) escaping from the QW to GaSb barriers, is expected to be important at temperatures higher than 300 K since the energy differences between the carrier confinement levels in the QW and the barrier become comparable or even less than the thermal energy at 300 K.

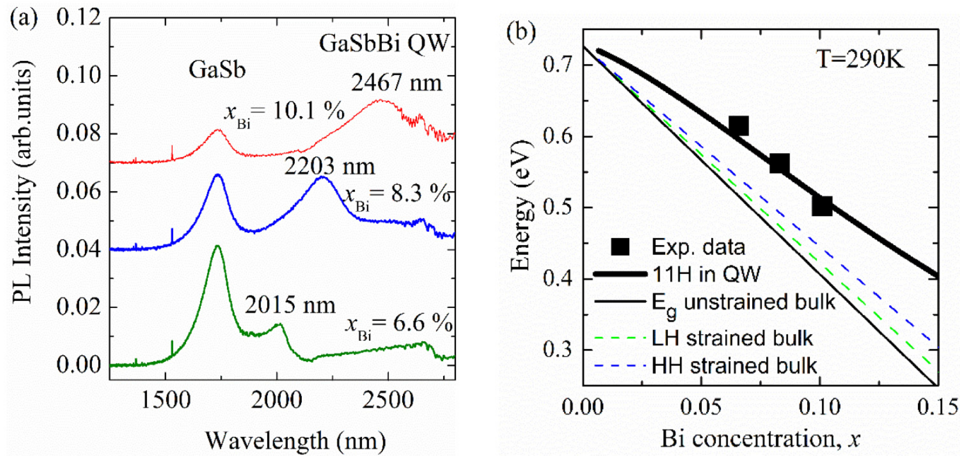

Fig. 4. (a) RT PL spectra of GaSbBi QW samples with varying Bi concentration. (b) Fundamental transition in the QW extracted from PL measurements (solid squares). Bandgap of unstrained GaSbBi (thin black line), light-hole (LH) strained bandgap (green dash line), heavy-hole (HH) strained band gap (blue dash line), and the fundamental transition (11H) in the GaSbBi/GaSb QW(thick black line) calculated using 8-band ***kp*** Hamiltonian.

Temperature dependent PL spectra were measured in the temperature range of 9−290 K for the three GaSbBi QW samples, as shown in Fig. 6. Two PL features were observed in the low temperature range of 9−150 K. The low energy PL peak is due to the band-to-band recombination in GaSbBi QW. The high energy PL peak at around 0.750 eV is attributed to the impurity-induced interband recombination in Te-doped GaSb substrate [22]. The PL peaks emitted from Te-doped GaSb substrates diminish and hardly redshift with the temperature rising, and eventually disappear at 190 K. Then, a weak PL peak appears on the high energy side as temperature is above 190 K. This weak PL peak is emitted from the GaSb buffer layer and capping layer. For the 6.6% Bi content sample, the PL intensity of GaSbBi QW is stronger than that of GaSb substrate. While for the 8.3% and 10.1% Bi content samples, the PL intensity is weaker than that of the GaSb substrate. It is obvious the PL peak of GaSbBi redshifts and becomes weak with rising temperature. The PL evolution with temperature will be discussed below.

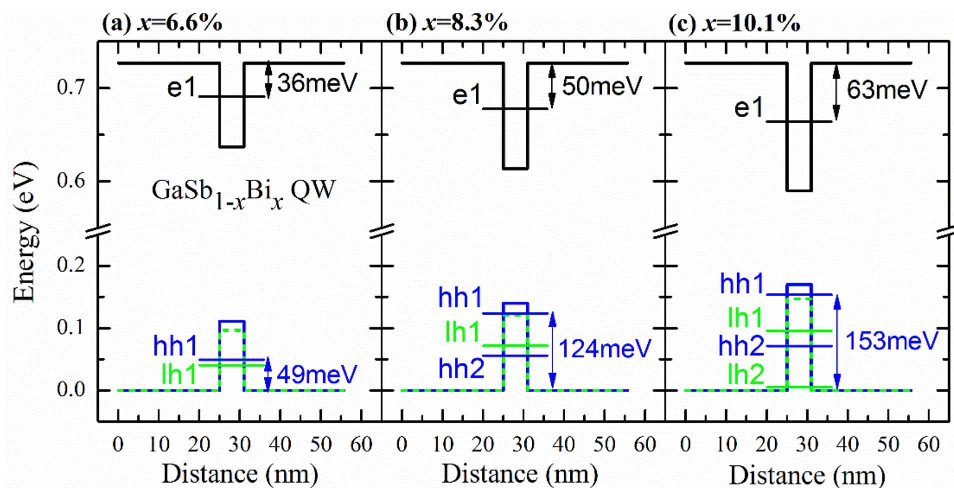

Fig. 5. Quantum confinement potential for GaSbBi/GaSb QWs of various Bi concentrations together with energy levels confinement in the QW.

Optical Materials EXPRESS

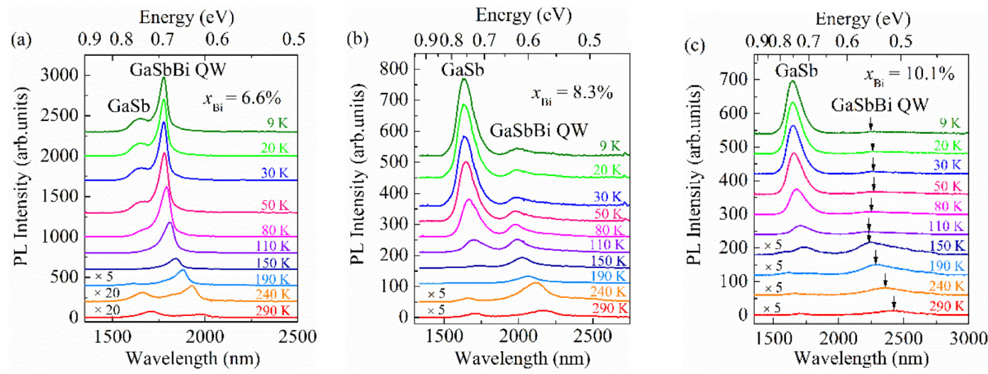

Fig. 6. Temperature dependence of PL spectra for GaSbBi QW samples with Bi content of (a) 6.6%, (b) 8.3% and (c) 10.1%. Black arrows are positioned in (c) to mark the PL peaks of GaSbBi QW.

Table 1.Varshni fitting parameters.

x_{Bi} (%)	E (0) (eV)	α (meV/K)	β
GaSb [2]	0.813	0.37	90
6.6	0.699	0.51	298
8.3	0.632	0.34	217
10.1	0.567	0.63	731

The temperature dependent PL peak energy of GaSbBi QWs is plotted in Fig. 7(a). The top dashed line is a Varshni fitting curve of GaSb using the reported parameters [2]. The data of GaSbBi are also fitted by Varshni's equation,

$$E(T) = E(0) - \alpha T^2 / (T + \beta), \tag{1}$$

where E (0) is the 0 K bandgap of GaSbBi, α and β are fitting parameters. These parameters are listed in Table 1. There is a deviation from Varshni's equation at the low temperature range for the 8.3% and 10.1% samples. The temperature dependent PL peak presents an S-shape behavior which becomes obvious with increasing Bi content. The S-shape is a signature of localized states due to the disorder caused by the Bi spatial composition fluctuations and Bi clusters induced by a high Bi concentration which have also been observed in GaAsBi [23–25] and InPBi [26]. The more the Bi atoms are incorporated in, the more the localized states are induced. At low temperatures, the low energy band-tails of the PL spectra are caused by the recombination of electron-hole pairs trapped in the localized states near the valence band maximum. In the low temperature range of 9 – 110 K, the PL spectra of the 8.3% and 10.1% Bi content GaSbBi QW show weaker intensity and broader FWHM than that of the 6.6% Bi content GaSbBi QW. At high temperatures, the carries have enough energy to become delocalized. The PL peak energy shows usual temperature-dependent redshift evolution. For the fitting parameters α and β, their values appear a rising tendency with increasing Bi content, except for the 8.3% Bi content. One possible reason for the deviation for the 8.3% Bi content sample is the experimental error due to the difficulty of accurately extracting the peak energy from a weak and broad PL peak. Another reason is that the sample with a high Bi content may have strong nonuniformity of Bi composition and Bi clusters and related complex point defects. In this case, the PL signal often contains multiple transitions and it is hard to retrieve transition energy between free electrons and holes confined in a QW. In the range of 110–290 K, the transition energy decreases with increasing temperature. The slope of the curve ΔE/ΔT is –0.32, –0.26 and - 0.23 meV/K for 6.6%, 8.3% and 10.1% Bi content

GaSbBi QW, respectively. The redshift rate of bandgap energy becomes slow with increasing Bi content, i.e. the temperature stability of GaSbBi QW is improved. Figure 7(b) shows the integral PL intensity evolution with temperature. The activation energy can be deduced by fitting the temperature dependent integral PL intensity curves using the equation [27],

$$I_{int}(T) = C / (1 + Ae^{-E_a/k_B T}) \tag{2}$$

where the I_{int} is the integrated PL intensity, A and C are the fitting constants, k_B is the Boltzmann constant, and T is temperature. The activation energy of the 6.6%, 8.3% and 10.1% Bi content GaSbBi QWs are deduced as 75 ± 10 meV, 81 ± 15 meV and 90 ± 10 meV, respectively. The activation energy increases with Bi content, demonstrating that the temperature stability of GaSbBi QW is improved with increasing Bi content. Although the fitted activation energies are larger than the calculated energy difference between the first electron level in the QW and the conduction band in GaSb barrier of 36, 50 and 63 meV, for the 6.6%, 8.3% and 10.1% Bi content GaSbBi QWs, respectively, both sets of the values have the similar trend.

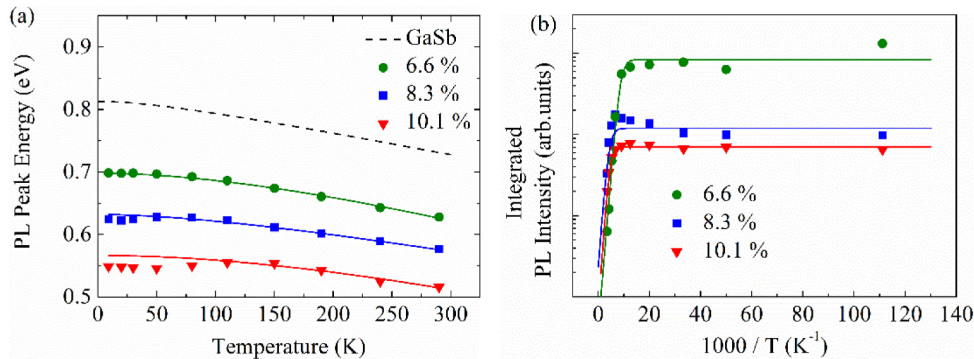

Fig. 7. (a) Temperature dependence of the PL peak energy and Varshni fitting curves of GaSbBi, and the Varshni fitting curve of GaSb using the parameter from reference [2]; (b) Temperature dependence of integrated PL intensity and the fitting curves using Eq. (2).

4. Summary

In summary, GaSbBi/GaSb QWs were grown with Bi contents up to 10.1%. HRTEM measurements confirm that the GaSbBi/GaSb QW structures have high crystalline quality and clear GaSbBi/GaSb interfaces. The incorporated Bi atoms are at substitutional sites and the Bi diffusion is found to be negligible. RT PL spectra reveal peak energy redshifts with increasing Bi content at about 32 meV/Bi%, reaching up to ~2.5 μm for 10.1% Bi content. The tansition energy in the GaSbBi/GaSb QW is calculated using the 8-band ***kp*** model and is consistent with the experimental results. The temperature dependent PL peak energy shows S-shape, indicating the presence of localized states in the GaSbBi QW. The temperature-insensitivity of GaSbBi QW is improved with increasing Bi content. These results demonstrate that GaSbBi QW has potentials for making mid-infrared opto-electronic devices.

Funding

National Basic Research Program of China (973 Project) (Grant No. 2014CB643902); the Key Program of Natural Science Foundation of China (Grant No. 61334004); the National Key Research Program of China (Grant No. 2017YFB0405300); Science and Technology Commission of Shanghai Municipality (Grant No.16ZR1441400); and the National Natural Science Foundation of China (Grant No. 61404152); Swedish Research Council (VR); NCN (grant no. 2013/10/E/ST3/00520).